15TH IEA HEAT PUMP CONFERENCE
MAY 26–29, 2026 | HOFBURG
VIENNA 2026
DECARBONISATION THROUGH INNOVATION

Performance evaluation of industrial heat pump based on reversed Stirling cycle for ultra-high temperature applications

Arne Høeg[a], Else Stougård Andersen[a], Kristian Løver[a], Rebekka Reberg[a], Ignat Tolstorebrov[b], Norbert Lümmen[c]

[a]Enerin AS, Asker, Norway
[b]Norwegian University of Science and Technology, Trondheim, Norway
[c]Western Norway University of Applied Sciences, Department of Mechanical Engineering and Maritime Studies, Bergen, Norway

Abstract

This paper presents comprehensive test results and performance evaluation of a 400-kW industrial heat pump operating on the reversed Stirling cycle. The system uses helium (R704) as the working fluid and can deliver heat at temperatures up to 200°C. Performance data collected from multiple installation sites in the food and pharmaceutical industries demonstrate the system's capabilities across various operating conditions.

The heat pumps have been operated with source temperatures ranging from 15°C to 68°C and sink temperatures ranging from 134°C to 199°C, corresponding to temperature ratios from 1.25 K/K to 1.55 K/K. Carnot efficiency is found to be a function of temperature ratio, and the heating capacity does not vary with the source temperature. The heat pumps have been operated for 15 000 hours in varying operating conditions, but the performance has been evaluated for periods with nearly steady operating conditions, in total 8 000 one-hour periods of steady conditions.

Results show significant efficiency advantages compared to conventional technologies for high temperature lifts. The measured performance data closely match simulation model predictions, validating the theoretical approach used for system design.

Keywords: Reversed stirling cycle; industrial heat pump; steam generating heat pump; HTHP; high temperature heat pump; helium; R704

1. Introduction

The HoegTemp industrial heat pump from Enerin AS is a reversed Stirling cycle heat pump, designed as a V6 with four process circuits arranged in a double-acting gamma configuration, with integrated heat exchangers for source and sink circuits. The heat pump has a rated heating capacity of 400 kW_{th} at sink temperatures up to 200°C and with source temperatures between -30°C and +130°C. The heat is delivered to a pressurized water circuit that can supply a steam generator, a water-heated boiler.

The heat pump is designed as a double-acting piston compressor, with 2 identical cylinder banks set in a 90° V configuration. Each cylinder bank consists of 3 cylinders with double-acting pistons, connected by gas ducts and heat exchanger modules. Figure 11 is from patent application NO 20220661 and shows a principal cross section through one cylinder bank. The centre piston 6 (the power piston) separates two circuits of a circuit pair, and each circuit consists of a displacer piston (5,7) in a displacer cylinder (D1, D2) and at least one heat exchanger module (1H, 2H). The displacer piston 5 separates a hot compression volume 1a above the piston from a cold expansion volume 1b below the piston. The circuit has nearly uniform pressure, and the piston configuration is such that the power piston increases the gas pressure and hence the gas temperature in one circuit when its displacer piston is in the lower position and reduces the gas pressure and hence the gas temperature in the circuit when its displacer is in the upper position. The displacer piston moves the gas through the heat exchangers with minimal pressure drop, so that hot gas will heat the upper heat exchanger 1he and cold gas will cool the lower heat exchanger 1hc. A regenerative heat exchanger 1hr is placed between the upper and lower heat exchanger, to store the heat while moving the gas between the hot and cold volume. Figure 1 shows the process of the 2 circuits in a circuit pair in a pv diagram. From Høeg et al [1].

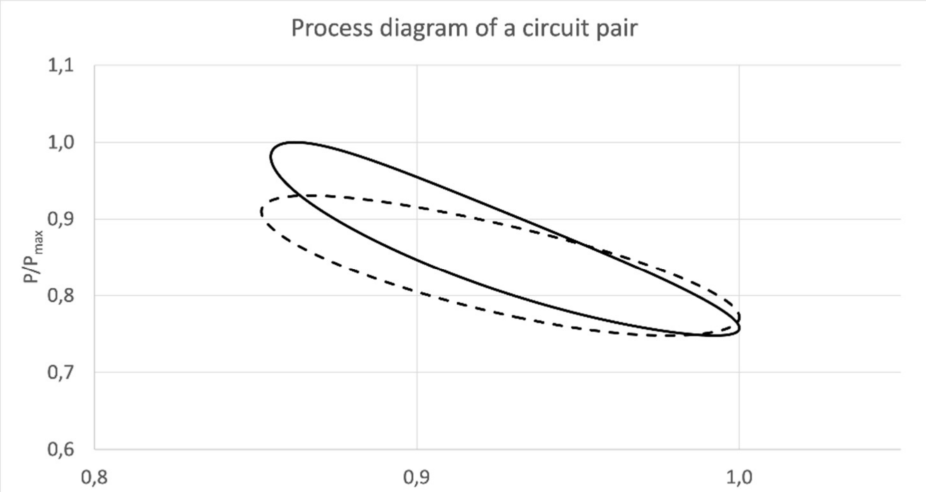

Figure 1. Pv diagram for the two circuits of a circuit pair in the HoegTemp heat pump

The heat pump uses pressurized helium (refrigerant R-704) as working medium and has a non-pressurized crankcase with oil-lubricated mechanicals, separated from the process by proprietary piston rod seals. The heat pump complies with EU's Machinery Directive and Pressure Equipment Directive, as well as other relevant directives and standards, such as EN 13445-3.

Three heat pumps have been installed so far: No. 1 at the IVAR biogas facility near Stavanger, Norway. No. 2 is located at the pharmaceutical plant of GE Healthcare, Lindesnes, Norway, and no. 3 at the seafood processing plant of Pelagia, Måløy, Norway. The first installation is described by Høeg et al. [1-2]. Figure 2 shows heat pump no. 2 at GE Healthcare.

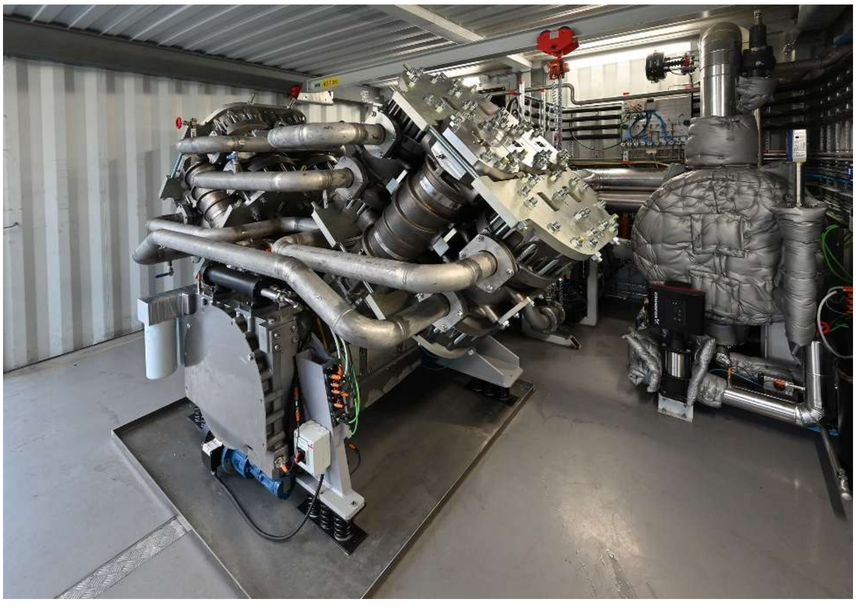

Figure 2. HoegTemp HTHP with steam generator, as installed at GE Healthcare, Lindesnes, Norway

2. Environmental advantages

In current installations, as well as future planned installations, the HoegTemp HTHP replaces either gas fired steam boilers, or electric steam boilers. With historical COPs of 1.6 or higher for the most recent installation at Pelagia Måløy, as shown in Figure 5, replacing these steam boilers with a HoegTemp HTHP enables significant reduction of CO_2 emissions.
As an example, the heat pump may replace industrial LPG boilers for steam production. Using an emission factor of 11,85 gCO_2/kWh [3] for electrical power consumption in Norway, and 230gCO_2/kWh for LPG [4], the heat pump installation will have an emission factor of 7,4gCO_2/ kWh_{th} while the LPG gas boiler has an emission factor of 230gCO_2/ $kWh_{th.}$of steam delivered. This is an emission reduction of 97%.

The European Union has a target of reducing carbon emissions by 55% [5] by 2030, and 90% by 2040. The estimated potential for delivering thermal energy in the EU using heat pumps is estimated to be 28 TWh per year for steam delivery at temperatures up to 150°C [6], and the potential delivery temperature of the HoegTemp HTHP of 250°C increases this even further. The potential up to 150°C equates to a potential CO_2 emission reduction of 62 million metric tons per year. With EU industrial emissions of approximately 500 [5] million metric tons in 2025, widespread adaptation of HTHPs in industrial processes may decrease the EU industrial CO_2 emissions by 12% yearly, as a major contributor to meeting the carbon emission reduction goal.

A secondary advantage of the heat pump is its contribution to security of energy supply for industry. Recent years have seen major challenges in energy supply, with geopolitical factors causing energy prices and supply of both fossil fuels and electricity to fluctuate.[7] As the heat pump replaces fossil fuels, or as an alternative to an electric boiler decreases use of electricity, implementing it may help the industry safeguard against a future energy market where both price and availability of energy carriers grow increasingly uncertain.

3. Process overview

Heat pumps no. 1 and 2 are connected directly to the heat source, in the form of pure water from a factory cooling system, as shown in Figure 3. A circulation pump draws a side-stream from the cooling circuit and pumps it through a series of heat exchangers on the cold side of the heat pump, before it is discharged back to the cooling circuit downstream of the extraction point. Tie-in to the factory cooling circuits is by two DN100 pipe connections on the existing piping. The heat source for heat pump no. 3 is in the form of product-contaminated condensate from the fish processing plant, available at high temperatures but low and varied flowrate. A heat exchanger is therefore used to transfer source heat to an intermediate water circuit, as shown in Figure 4. This protects the heat pump heat exchangers from fouling and enables a set flowrate through the heat pump, irrespective of heat source flow, ensuring good flow- and heat transfer conditions.

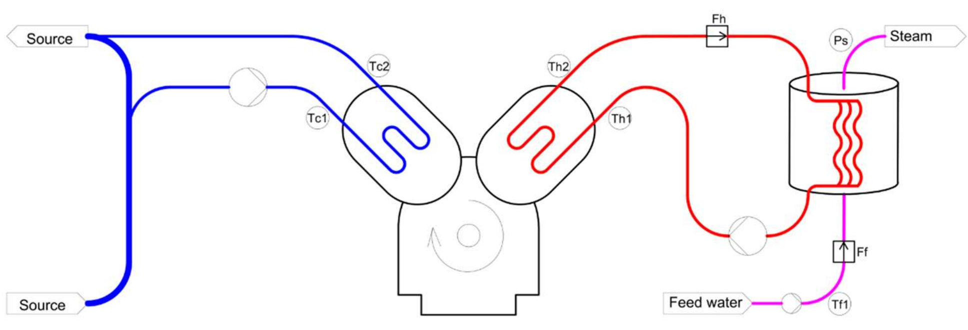

Figure 3. Schematic of HoegTemp HTHP no. 1 (IVAR) and no. 2 (GE)

On the sink side, the three heat pump systems share the same basic design. Heat produced by the heat pump is transferred to a closed and pressurized water circuit, with main dimension DN100, where a pump circulates the water between the heat pump and a steam generator. The steam generator is a shell and plate heat exchanger which produces steam by evaporation of feed water by heat transfer from the hot water circuit. The temperature in the hot water circuit is determined by the vaporization temperature in the steam generator.

Produced steam is fed into a factory steam line as a supplement to boiler steam. Consequently, the pressure in the steam generator is governed by the steam line pressure. Heat pump no. 1 (IVAR) has an option to throttle the steam delivery and thereby produce steam at higher pressure and higher hot water circuit temperature for testing purposes. For all three heat pumps, a feed water pump regulates the water level in the steam generator and maintains it at a constant level, feed water is supplied at close to saturation temperature through a DN25 tie-in pipe from either factory feed water tanks (no. 2 and 3), or a process condensate return line (no. 1).

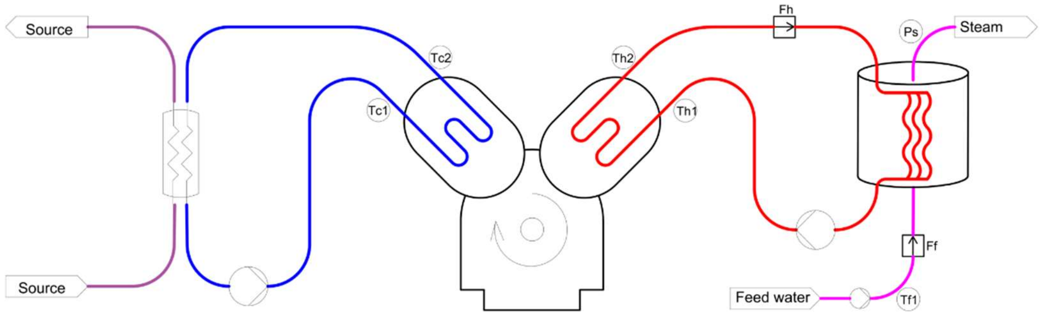

Figure 4. Schematic of HoegTemp HTHP No. 3 (Pelagia)

The hot water circuit of heat pump no. 1 is limited to 16 bar$_G$, limiting sink temperatures during testing to 200°C, while the water circuits of heat pumps no. 2 and 3 are limited to 6 and 12 bar$_G$, respectively.

A summary of the differences between the three installations is given in Table 1. The most important differences with respect to performance are assumed to be the piston configuration, the heat exchanger housing and the heat exchanger design. More specifically, the pistons are made from different alloys with different heat transfer properties, configuration B has lower conductivity. Heat exchanger housing B has slightly smaller heat conducting cross section between the hot and cold water circuits, and heat exchanger B has slightly modified surfaces compared to configuration A.

Table 1. Configuration overview of the 3 HoegTemp HTHP installations

Heat pump no.		**1**	**2**	**3**
Piston configuration		A	B	B
Heat exchanger housing		A	B	B
Heat exchanger design		A	A	B
Motor		Emit 250 kW 8-pole	ABB M3LP 400LB6	ABB M3LP 400LB6
VFD		ABB ACS880-07-0725A 400V	ABB ACS880-07-1140A 400V	ABB ACS880-07-0650A 690V
Heat source flow rate	kg/s	10 - 12	10 - 12	5 - 7.5
Hot-water flow rate	kg/s	15 - 20	15 - 20	15 - 20
Heat source typical glide	K	3	3	6
Hot-water typical glide	K	4	4	4
Feedwater temp	°C	104	97	110
Typical mean hot water temp	°C	139	137	163
Typical mean heat source temp	°C	28	25	40
Typical steam pressure	bar$_g$	2 - 2.2	1.9 - 2	5

4. Measurement and calculation of results

The heat source temperature, as referenced in this article, is taken as the average of heat pump inlet and outlet temperature (T_{c1}, T_{c2}) at the cold side. Similarly, the sink temperature is taken as the average of heat pump inlet and outlet temperature (T_{h1}, T_{h2}) at the hot side. The energy flow of produced steam, being the net output of the heat pump system, is calculated as the change in enthalpy between saturated water at temperature T_{f1} and saturated steam at pressure P_s, multiplied by mass flow F_f. This results in the following definition of COP (equation 1):

$$\mathrm{COP} = \frac{\dot{Q}_{\mathrm{steam}}}{\dot{W}_{\mathrm{mechanical}}} = \frac{F_f \cdot \left(h_{\mathrm{steam}}(P_s) - h_{\mathrm{feed}}(T_{f1})\right)}{\dot{W}_{\mathrm{mechanical}}} \qquad (1)$$

The direct energy output from the heat pump is calculated as the enthalpy change of water from inlet to outlet multiplied by mass flow F_h, and is without heat losses from piping, steam generator and associated equipment. It is however found that steam energy measurements provide higher consistency and serve as the preferred reference for COP calculation in this article.

Electric power consumption is measured by the variable frequency drive (ABB ACS880), controlling the heat pump electric motor. Mechanical power is then calculated by a fixed motor efficiency of 95.6% for heat pump no. 1, and by interpolation of motor efficiency data in the case of no. 2 and 3, where efficiency is a function of motor speed and load.

5. Measurement errors and verification of results

Instruments used to perform energy flow calculations, as well as their maximal measurement errors are shown in Table 1. Here, MV denotes the value measured by the instrument.

Table 2. Instrument measurement errors

Measurement	Sensor type	Maximal measurement error
Flow feed	IFM SU6020	0,02MV + 0,3 l / min
Temperature feed	IFM TA2415	0,3K + 0,001MV
Pressure steam	IFM PV8003	0,13 bar
Hot water flow	Heinrichs DVH-VW	0,007MV
Hot water temp	IFM TS2415	PT100 class A: 0.15+0.002|T| K

The validity of the steam energy flow measurements used in COP calculations can be assessed by comparing them to measured energy flow from the heat pump to the hot side circuit. These measurements are completely independent, with no common instrumentation. In Figure 5, the steam energy flow (x-axis) is plotted against the heat pump energy flow (y-axis), revealing a linear relationship for all three heat pumps. A positive constant term in the correlations is expected, representing heat losses from piping and the steam generator that are independent of energy flow. The given constants are however not accurate representations as they are heavily influenced by measurement errors and the limitations of the linear regression model.

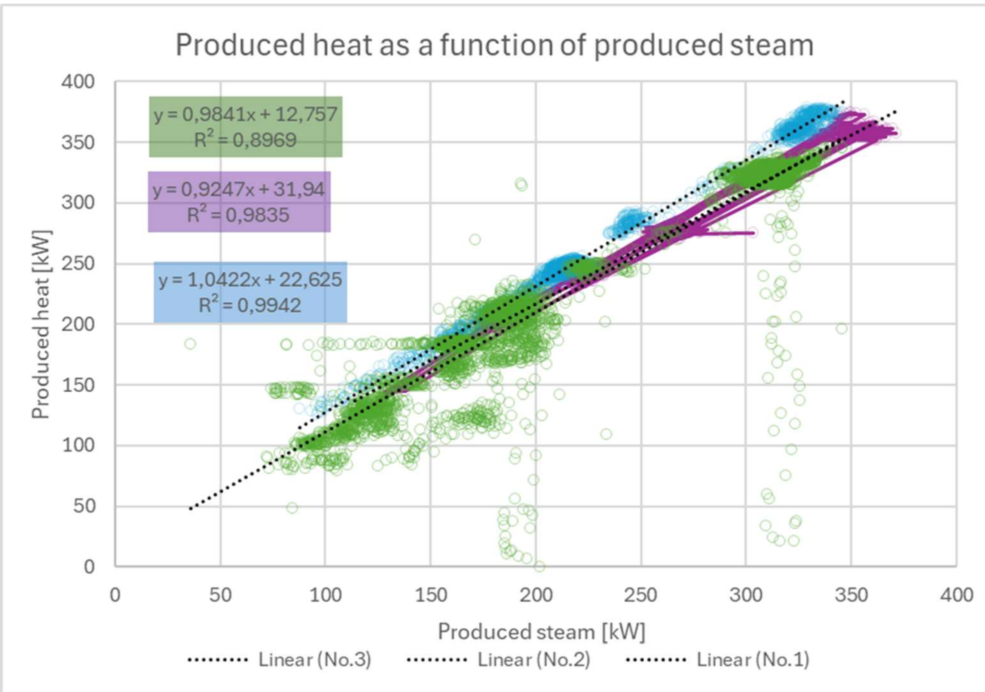

Figure 5. Produced heat in the hot circuit as a function of produced steam

6. Operation

The heat pumps have been operated with source temperatures ranging from 15°C to 68°C and sink temperatures ranging from 134°C to 199°C, corresponding to temperature ratios from 1.25 K/K to 1.55 K/K. The heat pumps have been operated at part load from 100 kW_{th} to 370 kW_{th}. Figure 6 shows the analyzed operating points, as well as lines indicating the temperature ratios 1.25 K/K and 1.55 K/K, to show that different operating points can result in the same temperature ratio.

The performance has been evaluated at constant operating conditions, filtered for hours where water temperatures have varied less than 5°C, charge pressure has varied less than 2 bar and shaft speed less than 10 RPM. The original logged data set with 1 second resolution is filtered and averaged to produce 8000 hour-averaged data points for analysis. Hours with different operating parameters, such as motor duty, charge pressure and water temperatures have been kept, as long as these remained stable within the measured interval. This results in a wider spread of data, and a higher standard deviation from each operating point to the regressed COP curve. Only conservative filtering of the data was performed, to best represent the real-world varying conditions where the heat pumps have been in operation.

The heat pumps have been tested during rapid temperature transients and with rapid load response, but these operating points have not been evaluated in this analysis. As per time of writing (November 2025), the heat pumps have been in operation for 15000 hours, combined.

Heat pump no. 1 has been operated with small variations in source temperature and with sink temperatures ranging from 134° to 199°C. Heat pump no. 2 has been operated at near constant source and sink temperatures, and heat pump no. 3 has been operated with varying heat source temperature and smaller variations in sink temperatures.

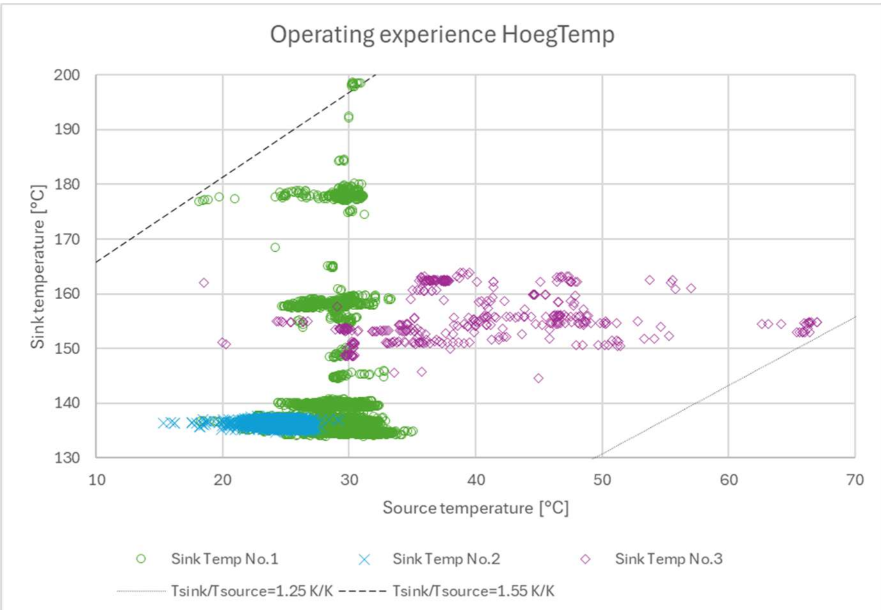

Figure 6. Operating points for 3 heat pump installations defined by sink temperature and source temperature

The COP of the ideal Stirling cycle, like the COP of the Carnot cycle, is a function of the ratio of the absolute sink and source temperature. Høeg et al. [1,2,8] have shown that the COP, and hence the Carnot efficiency, is mainly a function of the temperature ratio between the sink and source temperatures for real reversed Stirling cycle heat pumps. Figures 7 and 8 indicate that this is also the case for the HoegTemp heat pumps. Figure 7 indicates significant efficiency improvements from no. 1 to no. 2 to no. 3. This is the result of small changes to the heat pump parameters for each iteration, as summarized in Table 1. A logarithmic trendline (equation 2) has been found for Carnot efficiency for no. 3 in Figure 8, and this trendline has been used to create the trendline for COP in Figure 7.

$$\text{Carnot efficiency} \approx 0.6826 \ln\left(\frac{T_{\text{sink}}}{T_{\text{source}}}\right) + 0.3263 \qquad (2)$$

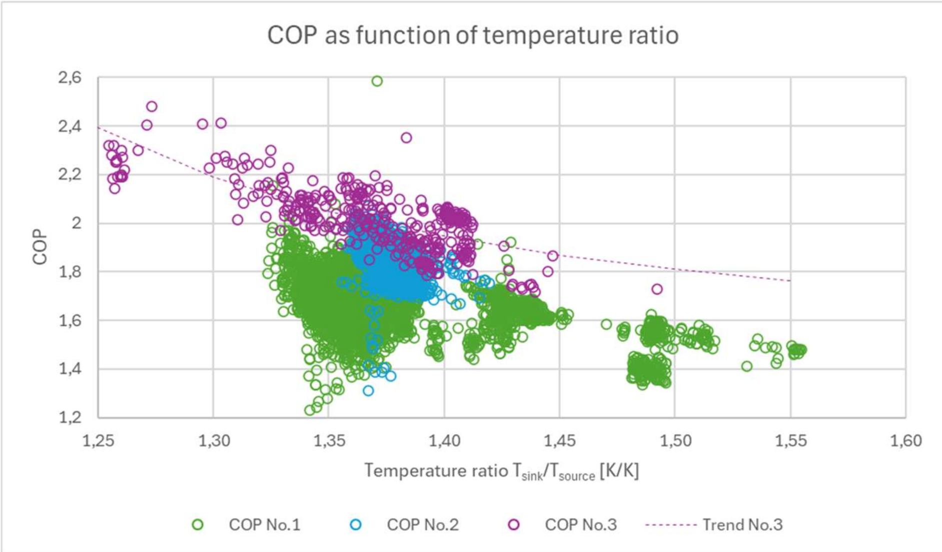

Figure 7. COP as a function of temperature ratio between sink and source

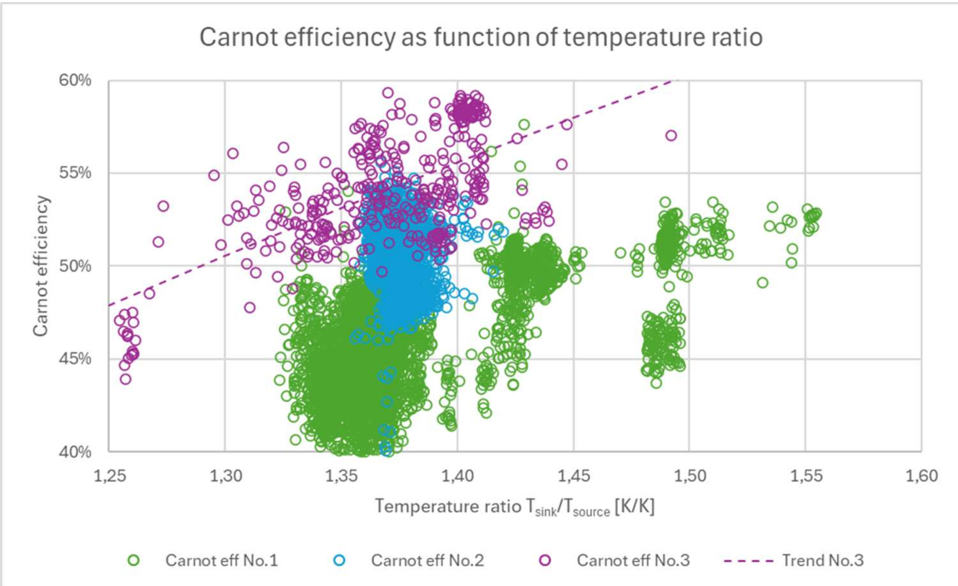

Figure 8. Carnot efficiency as function of temperature ratio between sink and source

Carnot efficiency is plotted as function of heating capacity for the three heat pumps in Figure 9. For all three heat pumps, efficiency varies with heating capacity, but the test data does not show a clear trend: No. 2 and no. 3 seem to have the highest Carnot efficiency at part load, while no. 1 seems to have the highest Carnot efficiency at close to rated capacity. The results may be distorted as a larger proportion of the test data for no. 1 at high output are at high temperature ratios that tend to have high Carnot efficiency. Part load efficiency is generally good.

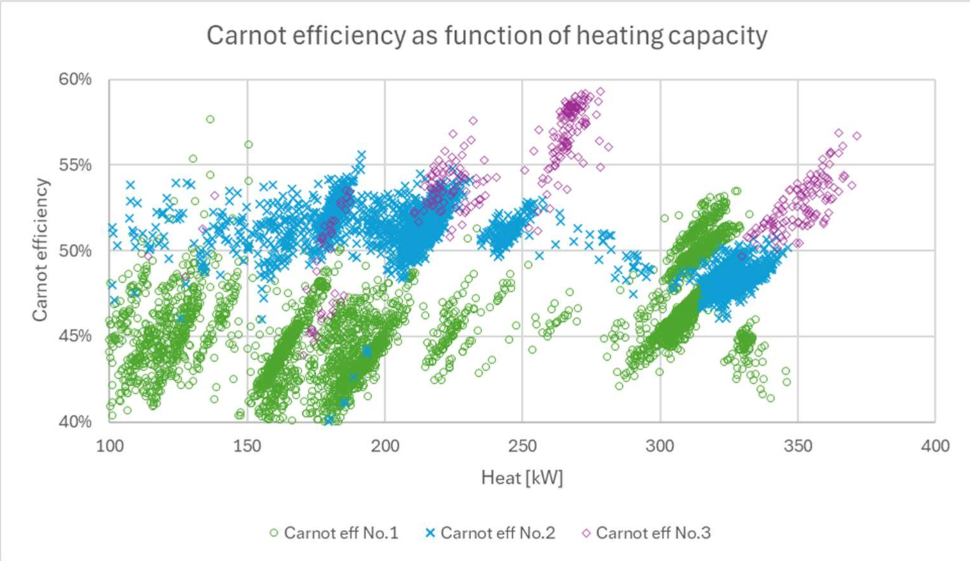

Figure 9. Carnot efficiency as function of heating capacity

Carnot efficiency increases with temperature ratio, even for electric boilers. The share of recycled heat, as represented by the ratio of cooling COP to Carnot cooling COP is another interesting metric. Figure 10 shows the efficiency of the heat pumps in terms of recycled heat (cooling). The Carnot cooling efficiency seems to have a maximum around 1.35 K/K of around 40% for heat pump no. 3.

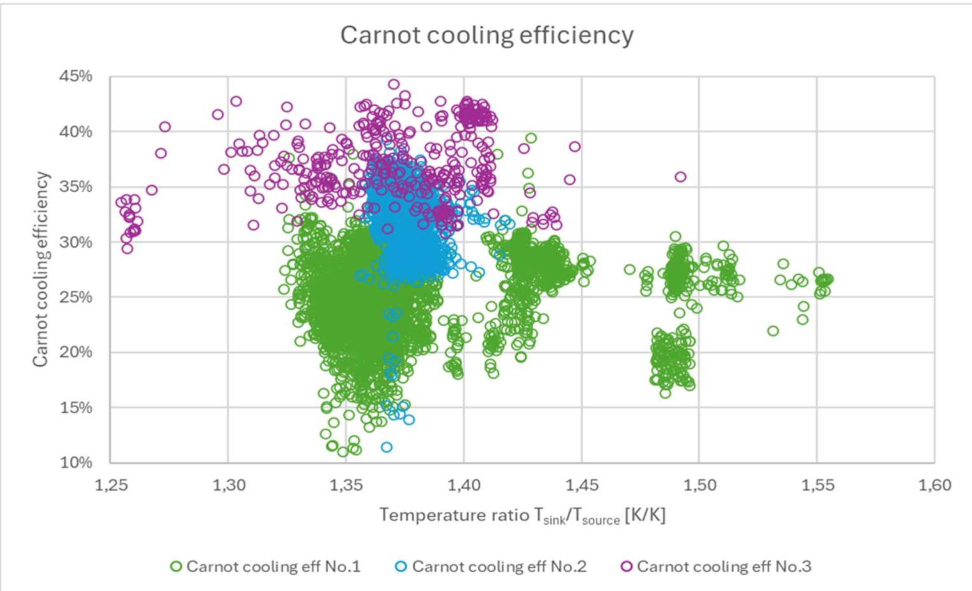

Figure 10. Efficiency of recycled heat

The three installations have had different operating conditions and challenges, resulting in experience and learning points: In the first installation, feedwater supply in the form of process condensate return was restricted, leading to cavitation issues when the feedwater temperature was high. The makeshift solution was to cool the feedwater to reduce the boiling risk. In the third installation, the main challenge has been to design the communication protocol between the plant management system and the heat pump control system so that the heat pump is operated optimally even when the plant operation is highly variable and intermittent.

7. Simulations

The heat pumps have been simulated using the 1-dimensional finite element model described in [1] and [2], with updated parameters, reflecting operating experience and minor modifications between the heat pumps.

The simulation model is modelled in the Stirling-cycle software SAGE (of Athens) with one pair of circuits modelled as connected control volumes. Friction and heat losses have been calculated analytically, and the results have been found in a spreadsheet for a V6 heat pump with 2 circuit pairs. Figure 11 shows the principal process components and control volume in a circuit pair, and Figure 12 shows the elements of the simulation model.

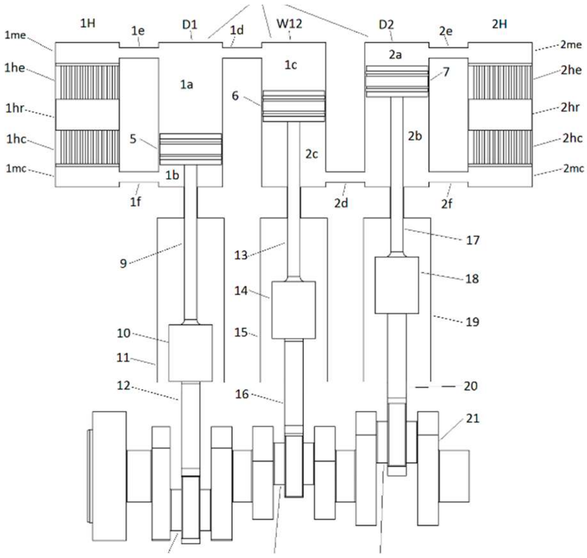

Figure 11. Process components of a circuit pair

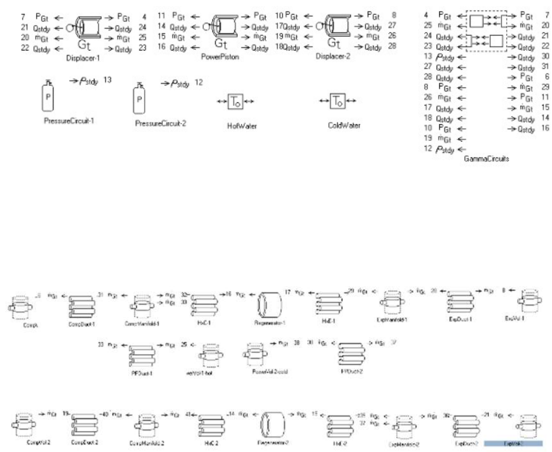

Figure 12. Simulation model

The simulation model has been run with parameters from heat pump no. 3 at Pelagia, at medium and high speed, for part load and high load. The simulation results are compared with the trend line from the measurements for heat pump no. 3, shown in Figure 13. The logarithmic trend line from the measurements is less curved than the simulation data. This may be because heat pump no. 3 has few data points at the extreme values of temperature ratio, or because a logarithmic trend line may not be the best choice of trend line.

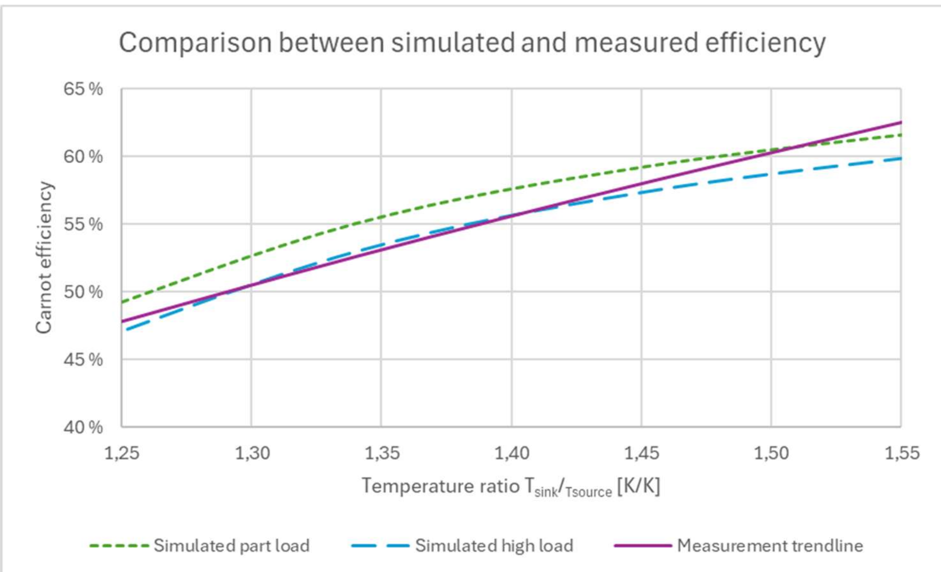

Figure 13. Comparison between simulated efficiency and trend line for measured efficiency

8. Conclusion

The trend line for Carnot efficiency for the HoegTemp is compared with peer reviewed and non-peer reviewed efficiency data for state-of-the-art heat pumps, as well as the reversed Stirling cycle heat pump HighLift from Single-Phase Power AS in Figure 14.

As the data in all previous charts have calculated COP and Carnot efficiency, using heat delivered to the steam and the shaft power as estimated by the VFD, the trendline must be adjusted for comparison with other heat pumps. The trendline from the research has been multiplied by the average efficiency of the motors at 96% to show the real-world efficiency of the heat pump with motor.

Peer reviewed heat pump performance data have been found from Bless et al. [9], Verdnik et al. [10] and Mateu-Royo et al. [6]. Performance data for the HighLift from SPP have been found from Hoeg et al. [8] and Bless et al. [9]. Non-peer reviewed supplier performance figures for high-temperature heat pumps have been found from Annex 58 [12] and from supplier presentations at IHPC 2025 [13]. Only data for heat pumps with sink temperatures of 120°C or higher have been included.

The comparison shows that the HoegTemp industrial heat pump, operating on the reversed Stirling cycle, with helium (R704) as refrigerant delivers competitive Carnot efficiency, especially for high temperature lifts above 1.3 K/K temperature ratio, or typically ΔT of 100°C or higher.

Høeg et al. [8] documents the performance of the HighLift heat pump from Single-Phase Power, in three installations from 2011 to 2015. This heat pump is also operated on the reversed Stirling cycle, using helium as refrigerant. This is the heat pump that is closest to the HoegTemp in process and operating conditions, and the comparison shows a clear efficiency improvement from this earlier design.

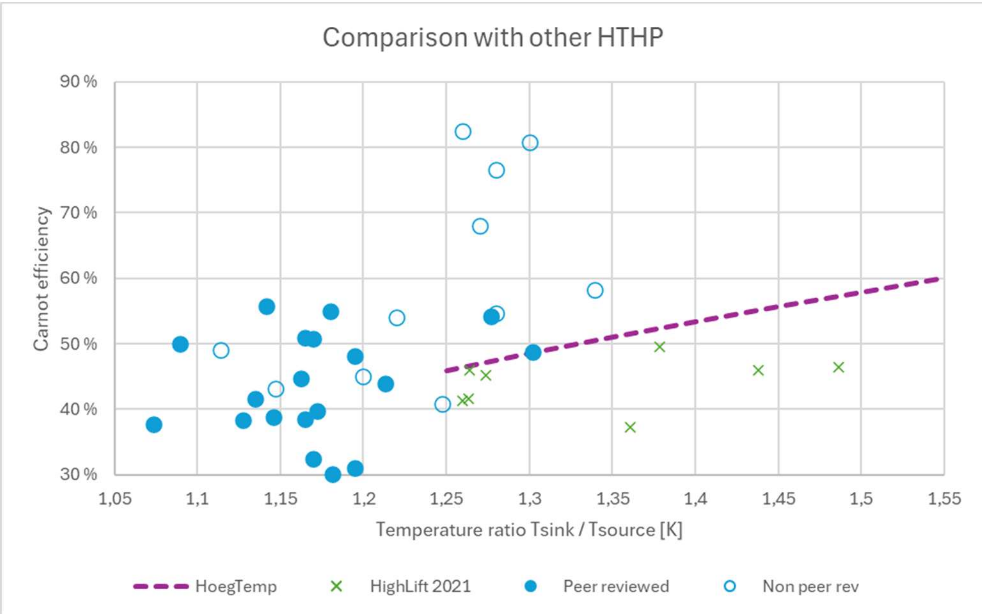

Figure 14. Carnot efficiency of HoegTemp compared with other heat pumps

Acknowledgements

The three heat pump installations have been partly funded by Innovation Norway (project no. 2020/540821) and Enova (project no. 22-9372 and 22-9361).

References

[1] Høeg A, Løver K, Asphjell, TA. *Performance of a new ultra-high temperature industrial heat pump*. 14th IEA Heat Pump Conference, USA, (2023).
[2] Høeg A, Løver K, Vartdal G. *Performance of a High-Temperature Industrial Heat Pump, using Helium as Refrigerant*. High-Temperature Heat Pump Symposium 2024, Denmark, (2024).
[3] NVE. *Strømdeklarasjoner.* Norwegian Water Resources and Energy Directorate (NVE), (2025).
[4] Miljødirektoratet. *Utslippsfaktorer i klimagassregnskap for Norge.* Norwegian Environment Agency (Miljødirektoratet), (2025).
[5] European Commission. *2040 climate target: Reducing the EU's net emissions by 90% by 2040.* EU Climate Action, (2025).
[6] Kosmadakis G, Papadopoulos A, Ntziachristos L, et al. *Estimating the potential of industrial (high-temperature) heat pumps for exploiting waste heat in EU industries*. Applied Thermal Engineering, (2019).
[7] International Energy Agency (IEA). *Global Energy Crisis.* IEA, (2025).

[8] Høeg A, Tveit TM. *Low to very high temperature thermal energy recycling – 3 case studies*. 19th International Stirling Engine Conference, Italy, (2021).
[9] Bless F, Arpagaus C, Bertsch S. *Theoretical investigation of high temperature heat pump cycles for steam generation*, 13th IEA heat pump conference, Jeju, Korea, 2020
[10] Verdnik M, & Rieberer R. (2022). *Experimental and model-based analysis of an R600 high-temperature heat pump in sub-critical and trans-critical operation.* 5th IIR-Gustav Lorentzen Conference on Natural Refrigerants – Manuscript ID 160
[11] Mateu-Royo C, Navarro-Esbrí J, Mota-Babiloni A, Molés F, & Amat-Albuixech M. (2019). *Thermodynamic analysis of a novel high-temperature heat pump for low-grade waste heat recovery*. Refrigeration Science and Technology Proceedings, 25th IIR International Congress of Refrigeration, Montreal, Canada.
[12] IEA Annex 58 – High temperature heat pumps. https://heatpumpingtechnologies.org/project58/. Date accessed: 17th November 2025.
[13] Industrial Heat Pump Conference 2025, Prague, Czech Republic.